HEPATOLOGY

A curcumin analog GL63 inhibits the malignant behaviors of hepatocellular carcinoma by inactivating the JAK2/STAT3 signaling pathway via the circular RNA zinc finger protein 83/microRNA-324-5p/cyclin-dependent kinase 16 axis

Ji-an Zhao,* Wenjia Nie,[†] Liang Dong,[†] Wencong Liu[‡] and Wei Wei[§] iD

Departments of *General Surgery, The First Hospital, [†]Medical Service, The First Hospital, [‡]Ultrasonography, The First Hospital, [§]Burn and Plastic Surgery, The First Hospital, Hebei Medical University, Shijiazhuang, China

Correspondence
Wei Wei, Department of Burn and Plastic Surgery, The First Hospital, Hebei Medical University, No. 89 Donggang Road, Shijiazhuang 050013, Hebei, China.
Email: ww18633889156@163.com

Abstract

Background and Aim: (1E,4E)-1,5-bis(2-bromophenyl) penta-1,4-dien-3-one (GL63) is a curcumin analog that can protect against carcinogenesis in hepatocellular carcinoma (HCC). The aim of this study was to explore the molecular mechanism of GL63 in HCC.
Methods: Cell viability was examined by cell counting kit-8 (CCK-8) assay. Circular RNA zinc finger protein 83 (circZNF83), microRNA-324-5p (miR-324-5p), and cyclin-dependent kinase 16 (CDK16) levels were measured via the quantitative real-time polymerase chain reaction (qRT-PCR). Cell proliferation was assessed using colony formation assay. Flow cytometry was performed for detecting cell cycle and apoptosis. Protein analysis was conducted by western blot. Cell migration and invasion were determined using transwell assay. Target relation was analyzed using dual-luciferase reporter and RNA immunoprecipitation (RIP) assays. The function of GL63 in vivo was researched by xenograft model in mice.
Results: GL63 inhibited the circZNF83 expression in HCC cells. CircZNF83 overexpression attenuated the inhibitory effects of GL63 on HCC cell growth, cell cycle progression, migration, and invasion but the promoting effect on cell apoptosis. CircZNF83 served as a sponge of miR-324-5p and circZNF83/miR-324-5p axis was involved in the functional regulation of GL63 in HCC progression. Moreover, CDK16 was a downstream target of miR-324-5p and circZNF83 could regulate the CDK16 expression by sponging miR-324-5p. The anti-tumor function of GL63 was also related to the miR-324-5p/CDK16 axis. In addition, GL63 inactivated the JAK2/STAT3 pathway via downregulating circZNF83 to mediate the miR-324-5p/CDK16 axis. GL63 also repressed tumor growth in vivo through the circZNF83/miR-324-5p/CDK16-mediated JAK2/STAT3 signal inhibition.
Conclusion: This study suggested GL63 impeded the HCC development by blocking the JAK2/STAT3 signaling pathway via mediating the circZNF83/miR-324-5p/CDK16 axis.

Introduction

Hepatocellular carcinoma (HCC) is the most common subtype of primary liver tumors with more than 800 000 new cases each year, and it is the fourth leading cause of human death from cancer all over the world.[1,2] Curcumin (CUR) is a natural phenolic compound with various pharmacological activities, such as anti-tumor, anti-inflammation, and anti-oxidation.[3] CUR was also used to inhibit the tumor developing process in HCC treatment.[4] Nevertheless, the clinical application of CUR was limited due to its low solubility and instability.[5,6] The synthetic structural analogs of CUR have been developed to improve the poor bioavailability of CUR in tumor treatment. (1E,4E)-1,5-bis(2-bromophenyl) penta-1,4-dien-3-one (GL63) is a novel analog of CUR, and it exhibits

antitumor activity in HCC.[7,8] However, the functional mechanism of GL63 in the HCC progression is unclear.

Noncoding RNAs (ncRNAs) including circular RNAs (circRNAs) and microRNAs (miRNAs) act as vital roles in tumor occurrence, progression, and chemoresistance in HCC.[9] CircRNAs are produced by back-splicing of pre-messenger RNAs (pre-mRNAs), and they have tissue/cell-specific expression patterns in eukaryotes.[10] CircRNAs can function as "sponges" to reduce the miRNA activities, thereby resulting in the regulation of downstream genes or signaling pathways.[10,11] The relation of circRNA and GL63 has never been researched.

A previous study indicated that circRNA zinc finger protein 83 (circZNF83, hsa_circ_0052112) promoted cell migration and

invasion in breast cancer by functioning as a miR-125a-5p sponge.[12] Luo *et al.* have reported the abnormal upregulation of circZNF83 in HCC patient samples.[13] Dysregulated expression of circRNA has crucial regulation in the development of cancer,[14] implying that circZNF83 might be involved in the HCC progression. Furthermore, whether circZNF83 is related to the function of GL63 in HCC remains to be explored. In addition, Cao *et al.* declared that microRNA-324-5p (miR-324-5p) repressed migration of HCC cells by targeting ETS1 and SP2.[15] Cyclin-dependent kinase 16 (CDK16) was an oncogene in HCC and circ_1306 could promote cell growth in HCC by sponging miR-584-5p to increase the CDK16 expression.[16] It remains unknown whether circZNF83 can regulate the level of CDK16 through the sponge effect on miR-324-5p.

Janus activated kinase 2 (JAK2) and downstream signal transducer/activator of transcription 3 (STAT3) are an important pathway in the development of HCC. For instance, cantharidin reduced cell viability and colony formation ability of HCC cells through the JAK2/STAT3 signal inhibition.[17] CircSOD2 contributed to the HCC progression by targeting the miR-502-5p/DNMT3a axis to activate the JAK2/STAT3 pathway.[18] Also, GL63 has suppressed cell proliferation by blocking the JAK2/STAT3 signaling pathway in HCC cells.[7]

This study concentrated on the anti-tumor mechanism of GL63 in HCC. We have investigated the potential regulation of circZNF83 on CDK16 via targeting miR-324-5p and the effect of circZNF83/miR-324-5p/CDK16 axis on the JAK2/STAT3 signaling pathway.

Methods

Tissue specimens. Hepatocellular carcinoma tissues ($n = 42$) and normal para-carcinoma tissues ($n = 42$) were acquired from 42 HCC patients at The First Hospital, Hebei Medical University. The written informed consent form was provided by each patient. All tissue specimens were saved in liquid nitrogen until further use. The procedures of this study were ratified by the Ethics Committee of The First Hospital, Hebei Medical University.

Cell culture and GL63 treatment. Human liver epithelial cell line THLE-2 and HCC cell lines (HuH-7, HCCLM3) were purchased from JENNIO (Guangzhou, China). Cells were cultured with Dulbecco's modified eagle medium (DMEM; Sigma-Aldrich, St. Louis, MO, USA) containing 10% heat-inactivated fetal bovine serum (FBS; Sigma-Aldrich) and 1% penicillin/streptomycin solution (Sigma-Aldrich) in a 5% CO_2 incubator at 37°C. GL63 was synthesized as previously reported,[8,19] and it was dissolved in dimethylsulfoxide (DMSO; Invitrogen, Carlsbad, CA, USA). Then HCC cells were respectively exposed to 10, 20, and 40 μM GL63 for 24 h.

Cell counting kit-8 (CCK-8) assay. The 96-well plates were seeded with HuH-7 and HCCLM3 cells at a density of 2×10^3 cells per well, and cells were cultured for 24 h to 70% coverage. After cells were treated with GL63, 10 μL per well CCK-8 reagent (Sigma-Aldrich) was added into the well-plates. Cell absorbance of 450 nm was determined under a microplate absorbancy reader (Sigma-Aldrich).

The quantitative real-time polymerase chain reaction (qRT-PCR) assay. TRIzol™ Reagent (Invitrogen) was adopted for isolating the total RNA from human tissues and cells. The first-strand complementary DNA (cDNA) was synthesized using ReverTra Ace® qPCR RT Kit (Toyobo, Kita-Ku, Osaka, Japan), and the real-time PCR was performed using SYBR® Green Realtime PCR Master Mix (Toyobo). The relative expression level was calculated by the $2^{-\Delta\Delta Ct}$ method. Glyceraldehyde-phosphate dehydrogenase (GAPDH) served as the reference gene for circZNF83 and CDK16, and the miR-324-5p expression was normalized by U6. The primers were shown as below: CircZNF83 (forward, 5ʹ-GAGGAGTGGAAATGCC TGAA-3ʹ; reverse, 5ʹ-CTGAGGAAGAGCCATCCTTG-3ʹ), miR-324-5p (forward, 5ʹ-GCCGAGCGCATCCCCTAGGG-3ʹ; reverse, 5ʹ-CAGTGCGTGTCGTGGAGT-3ʹ), CDK16 (forward, 5ʹ-CCGT CGTGTCAGCCTATCT-3ʹ; reverse, 5ʹ-CTTCTCCGTGTGGATA ATGTCA-3ʹ), GAPDH (forward, 5ʹ-GCACCGTCAAGGCTGA GAAC-3ʹ; reverse, 5ʹ-TGGTGAAGACGCCAGTGGA-3ʹ) and U6 (forward, 5ʹ-CTCGCTTCGGCAGCACA-3ʹ; reverse, 5ʹ-AACGCTTCACGAATTTGCGT-3ʹ).

Cell transfection. The sequence of circZNF83 was amplified and cloned into pcD5-ciR vector (vector; GENESEED, Guangzhou, China) to construct the pcD5-ciR-circZNF83 (circZNF83). MiR-324-5p mimic (miR-324-5p), miR-324-5p inhibitor (anti-miR-324-5p), small interfering RNA (siRNA) of CDK16 (si-CDK16), and the corresponding negative controls (miR-NC, anti-miR-NC, si-NC) were bought from Ribobio (Guangzhou, China). RNA or plasmid was transfected into the monolayer HuH-7 and HCCLM3 cells by Lipofectamine™ 3000 (Invitrogen).

Colony formation assay. HuH-7 and HCCLM3 were respectively seeded onto the 12-well plates with 200 cells per well. Cells were incubated at 37°C for 14 days. Subsequently, cell colonies were fixated with methanol (Sigma-Aldrich) and stained with 0.1% crystal violet (Sigma-Aldrich). The colonies were counted by arbitrary three fields under the microscope (Thermo Fisher Scientific).

Cell cycle analysis. Cell cycle progression was analyzed using Cell Cycle Assay Kit (Dojindo, Kumamoto, Japan); 2×10^5 cells were incubated with 1 mL ice-cold 70% ethanol (Sigma-Aldrich) at 4°C for 2 h. Then ethanol was removed, and cells were washed with phosphate buffer solution (PBS; Gibco, Carlsbad, CA, USA). Cells were added with 0.5 mL Working Solution at 37°C for 30 min and 4°C for 30 min, followed by cell detection on the flow cytometer (BD Biosciences, San Diego, CA, USA).

Flow cytometric analysis. Cell apoptotic rate was determined using Annexin V Apoptosis Detection Kit (Dojindo). Cells were digested with trypsin (Gibco), and cell pellets were resuspended in 1× Annexin V binding buffer. Then 1×10^5 cells were stained with 5 μL Annexin V-fluorescein isothiocyanate (FITC)

and 5 μL propidium iodide (PI) at room temperature for 15 min. Cell analysis was performed through the flow cytometer (BD Biosciences).

Western blot. Radioimmunoprecipitation assay lysis buffer (Millipore, Billerica, MA, USA) was used to extract the total protein, as per the user's manual book. The operating procedures were in accordance with the report of Lai *et al.*[20] The primary antibodies from Abcam (Cambridge, MA, USA) were exhibited as follows: anti-B-cell lymphoma-2 (anti-Bcl-2; ab32124, 1:1000), anti-Bcl-2 associated X (anti-Bax; ab32503, 1:1000), anti-cleaved-caspase-3 (ab2302, 1:1000), anti-CDK16 (ab15467, 1:1000), anti-JAK2 (ab108596, 1:1000), anti-phosphorylated-JAK2 (anti-p-JAK2; ab32101, 1:1000), anti-STAT3 (ab32500, 1:100), anti-phosphorylated-STAT3 (anti-p-STAT3; ab76315, 1:1000), and anti-GAPDH (ab181602, 1:3000). After the incubation with anti-rabbit IgG, HRP-linked secondary antibody (ab205718, 1:5000), the protein blots were visualized on the membranes using ECL Ultra Western HRP Substrate (Millipore). Data analysis was completed by ImageLab software version 4.1 (Bio-Rad, Hercules, CA, USA).

Transwell assay. For cell migration, the transwell chamber (12-well; Corning Inc., Corning, NY, USA) was planted with 2×10^4 cells in the upper chamber, and the low chamber was filled with 10% FBS + DMEM medium. After incubation at 37°C 24 h, cells remaining in the upper chamber were discarded, and cells passed into the lower chamber were fixated in methanol (Sigma-Aldrich). Then the fixated cells were stained with 0.1% crystal violet (Sigma-Aldrich), and cell number was counted by a microscope (Olympus, Tokyo, Japan). For cell invasion,

2×10^5 cells were inoculated onto the upper chamber coated with matrigel (Corning Inc.), and the other operations were conducted as per the migration assay. The images of migrated and invaded cells were acquired at 100× magnification.

Dual-luciferase reporter assay. The sequences of circZNF83 (wild-type, WT), mutated circZNF83 (MUT), CDK16 3ʹUTR (WT), and mutated CDK16 3ʹUTR (MUT) were cloned into the pmirGLO vector (Promega, Madison, WI, USA). The generated luciferase vectors for circZNF83 (circZNF83 WT, circZNF83 MUT), and CDK16 (CDK16 3ʹUTR WT, CDK16 3ʹUTR MUT) were respectively co-transfected with miR-324-5p or miR-NC into HuH-7 and HCCLM3 cells; 48 h later, the luciferase activity was examined using dual-luciferase reporter assay kit (Promega) according to the manufacturer's protocols.

RNA immunoprecipitation (RIP) assay. Protein A magnetic beads (Millipore) were pre-coated with anti-Argonaute-2 (anti-Ago2) or anti-immunoglobulin G (anti-IgG). HCC cells were lysed in RIP lysis Buffer (Millipore), and cell lysates were incubated with the antibody-coated magnetic beads at 4°C overnight. Whereafter, the magnetic beads were washed with PBS (Gibco), and the immunoprecipitated RNAs on the magnetic beads were purified. Then circZNF83 and miR-324-5p expression levels were detected via qRT-PCR. Cell lysates that were unincubated with magnetic beads were used as the positive control (Input).

Tumor xenograft assay. BALB/c male nude mice (5–6 weeks old) from Vital River Laboratory Animal Technology Co., Ltd. (Beijing, China) were cared in the specific-pathogen-free (SPF) environment with enough food and water. This assay was
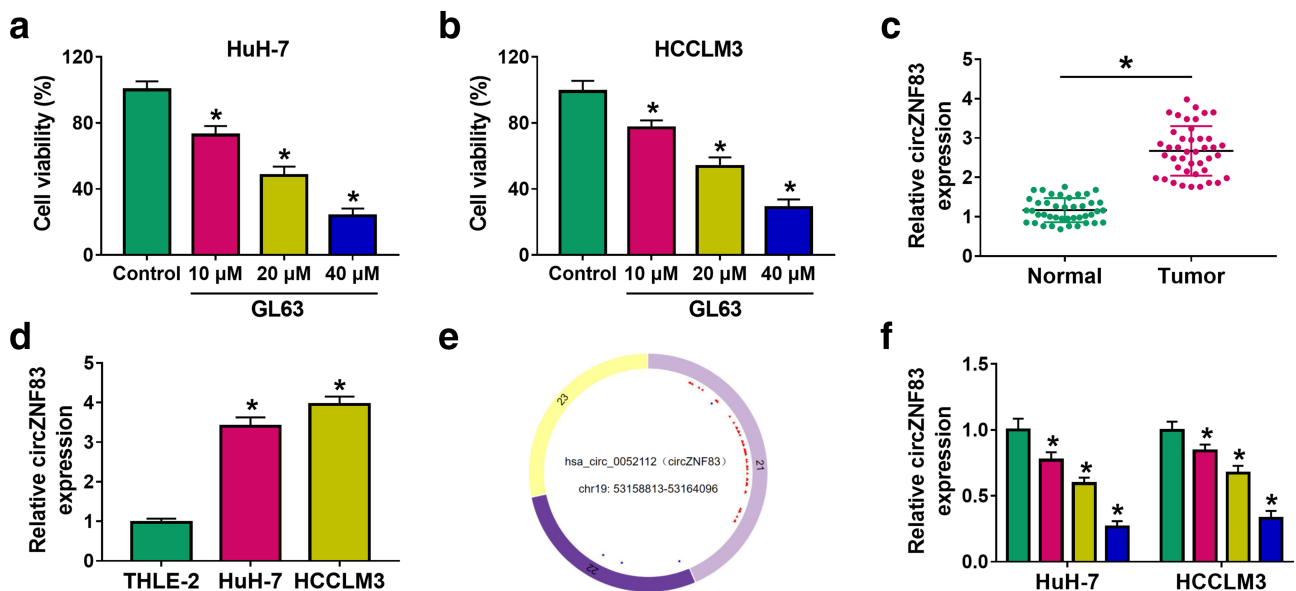

Figure 1 CircZNF83 expression was downregulated by GL63 in HCC cells. (a and b) Cell viability was measured via CCK-8 assay after HuH-7 (a) and HCCLM3 (b) cells were treated with 10, 20, or 40 μM GL63. (c and d) CircZNF83 expression was quantified using qRT-PCR in tissues (c) and cells (d). (e) CircZNF83 originates from the exon 21–23 of ZNF83 gene. (f) The effect of GL63 on the level of circZNF83 was analyzed using qRT-PCR. ■, Control; ■, 10 μM; ■, 20 μM; ■, 40 μM. *$P < 0.05$.

approved by the Animal Ethical Committee of The First Hospital, Hebei Medical University. These mice were arbitrarily divided into three groups (vector, GL63 + vector, and GL63 + circZNF83), with five mice per group; 1×10^7 HuH-7 cells with stable expression of vector or circZNF83 were subcutaneously injected into mice, followed by the intraperitoneal injection of 80 mg/kg GL63 twice a week. The length and width of tumors in mice were measured every week, and the growth curve of tumor volume (length × width²/2) was plotted. Seven weeks later, all mice were euthanized using CO_2 asphyxia method. Tumors were dissected from mice, and tumor weight was measured on an electronic scale. The RNA (circZNF83a and miR-324-5p) and protein (CDK16, p-JAK2, JAK2, p-STAT3, and STAT3) levels were determined using qRT-PCR or western blot.

Statistical analysis. SPSS 22.0 (SPSS Inc., Chicago, IL, USA) was used for the analysis of statistical data. Data were
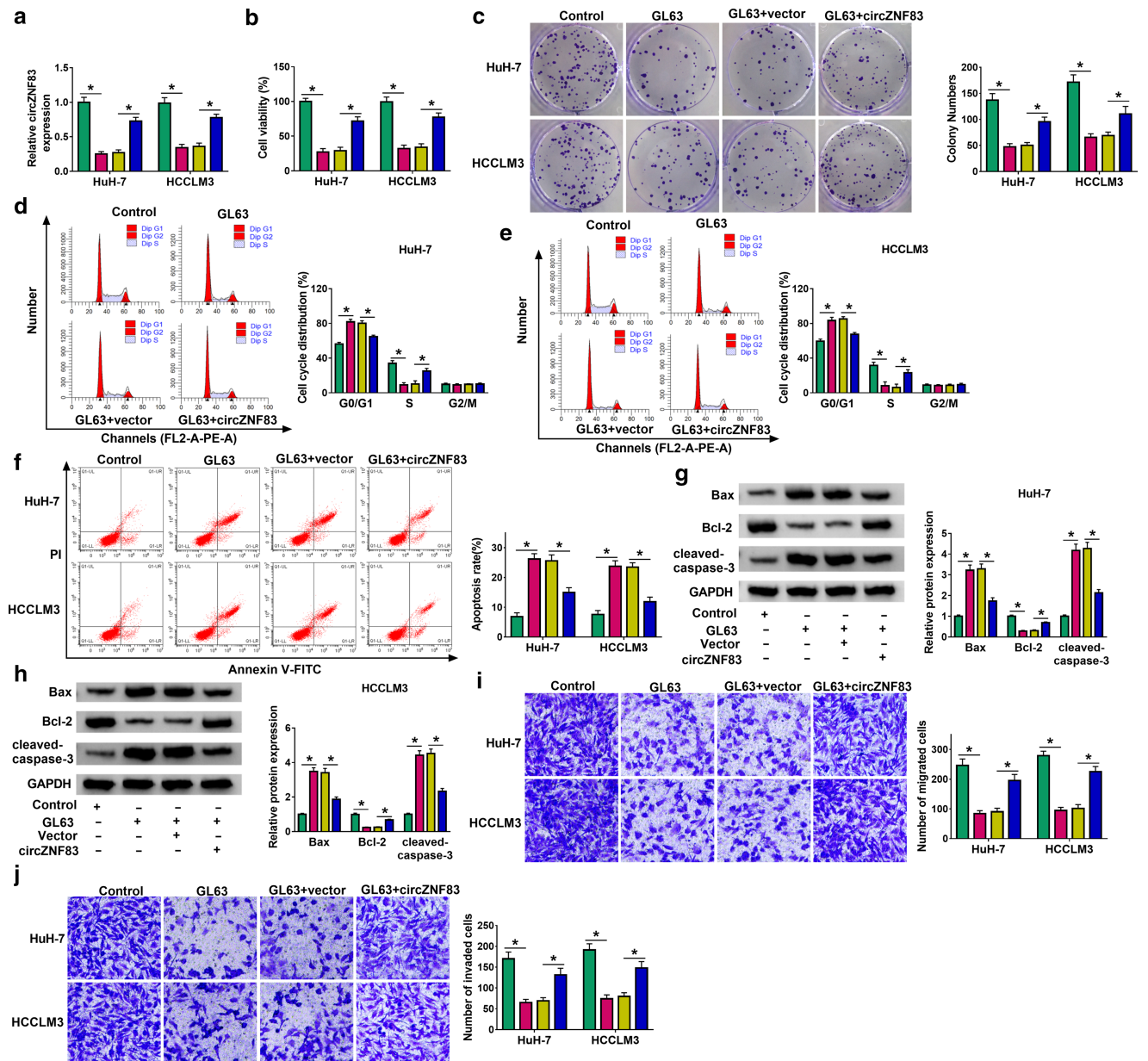

Figure 2 Overexpression of circZNF83 reversed the anti-tumor function of GL63 in HCC cells. Four groups (Control, GL63, GL63 + vector, and GL63 + circZNF83) were set in HuH-7 and HCCLM3 cells. (a) The qRT-PCR was used for the examination of circZNF83 expression. (b) CCK-8 assay was used for the detection of cell viability. (c) Colony formation assay was used for the analysis of cell proliferation. (d–f) Flow cytometry was used for the assessment of cell cycle (d and e) and cell apoptosis (f). (g and h) Western blot was used for the determination of apoptotic makers. (i and j) Transwell assay was used for the evaluation of cell migration (i) and invasion (j). *$P < 0.05$. (a–j) ■, Control; ■, GL63; ■, GL63 + vector; ■, GL63 + circZNF83.
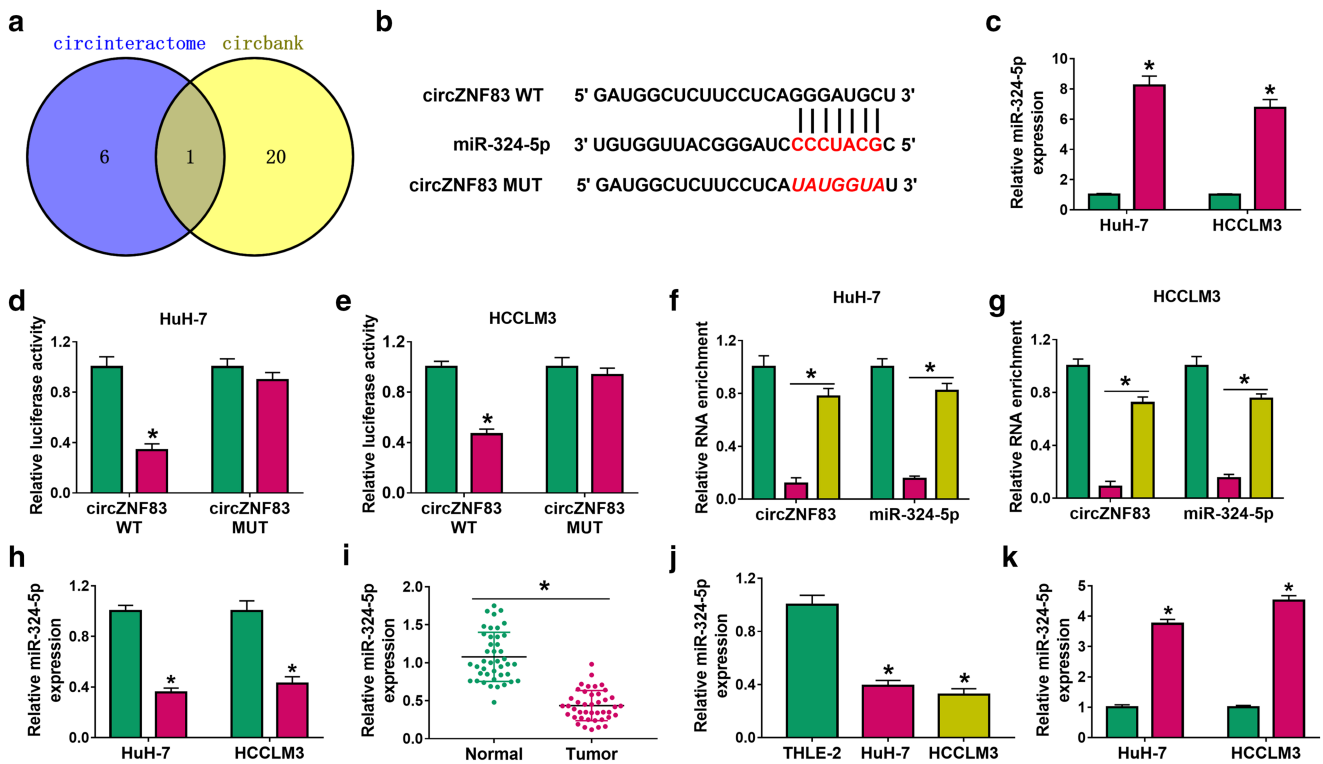
Figure 3 CircZNF83 targeted miR-324-5p in HCC cells. (a) Veen diagram analysis was performed to select the candidate target of circZNF83 from the predicted miRNAs by circinteractome and circbank. (b) Circinteractome showed the binding sites between circZNF83 and miR-324-5p. (c) The miR-324-5p expression was detected by qRT-PCR after transfection of miR-NC or miR-324-5p. (d–g) The binding between circZNF83 and miR-324-5p was validated by the dual-luciferase reporter assay (d and e) and RIP assay (f and g). (h) The effect of circZNF83 on the miR-324-5p level was analyzed by qRT-PCR. (i–k) The expression level of miR-324-5p was tested by qRT-PCR in tissues (i), cells (j), and GL63-treated HuH-7/HCCLM3 cells (k). *$P < 0.05$. (c–e) ■, miR-NC; ■, miR-324-5p. (f and g) ■, Input; ■, anti-IgG; ■, anti-Ago2. (h) ■, vector; ■, circZNF83. (k) ■, Control; ■, GL63.

derived from three independent experiments and represented as the mean ± standard deviation (SD). The difference between two groups or multiple groups was respectively analyzed using Student's *t*-test and one-way analysis of variance (ANOVA) followed by Tukey's test. $P < 0.05$ indicated that the difference was statistically significant.

Results

CircZNF83 expression was downregulated by GL63 in HCC cells.

GL63 has been reported to inhibit HCC cell growth in a dose-dependent manner.[7] HuH-7 and HCCLM3 cells were treated with GL63 (10, 20, and 40 μM) for 24 h, and then cell viability was detected by CCK-8 assay. The results affirmed that cell viability was reduced by different concentrations of GL63 in a dose-dependent way (Fig. 1a,b). The qRT-PCR assay demonstrated that the level of circZNF83 was much higher in HCC tissue samples (Fig. 1c) and HuH-7/HCCLM3 cell lines (Fig. 1d) than that in normal samples and THLE-2 cell line. CircZNF83 (hsa_circ_0052112) is an exonic circRNA from the exon 21–23 of ZNF83 gene, and it locates on the chr19: 53158813-53164096 with the spliced mature length of 209 bp (Fig. 1e). GL63 treatment resulted in the downregulation of circZNF83 expression in HuH-7 and HCCLM3 cells, and the

effect of 40 μM GL63 was the most conspicuous (Fig. 1f). The abnormal expression of circZNF83 induced by GL63 suggested that circZNF83 might be involved in the regulation of GL63 in HCC.

Overexpression of circZNF83 reversed the anti-tumor function of GL63 in HCC cells.

The function of circZNF83 was investigated in HCC cells under the treatment of 40 μM GL63. The circZNF83 expression was increased in GL63 + circZNF83 group relative to GL63 + vector group, indicating that the overexpression efficiency of circZNF83 transfection was significant (Fig. 2a). GL63-induced repressive effects on cell viability (Fig. 2b) and colony formation ability (Fig. 2c) were partly attenuated by circZNF83 overexpression. GL63 has blocked cell transition from G0/G1 phase to S phase in HuH-7 and HCCLM3 cells, whereas transfection of circZNF83 weakened the cell cycle arrest (Fig. 2d,e). Flow cytometry showed that the pro-apoptotic function of GL63 was abolished by the upregulation of circZNF83 (Fig. 2f). The apoptosis-associated proteins were further determined using western blot. As Figure 2g,h depicted, the introduction of circZNF83 mitigated the GL63-mediated downregulation of anti-apoptotic Bcl-2 but upregulation of pro-apoptotic Bax and cleaved-caspase-3. Additionally, circZNF83 enhanced cell migration (Fig. 2i) and

invasion (Fig. 2j) after HuH-7 and HCCLM3 cells were treated with GL63. Evidently, the anti-tumor function of GL63 in HCC was partly achieved by downregulating the expression of circZNF83.

CircZNF83 targeted miR-324-5p in HCC cells. The online circinteractome (https://circinteractome.nia.nih.gov/) and circbank (http://www.circbank.cn/index.html) were used for predicting the candidate targets for circZNF83. Veen diagram analysis revealed that miR-324-5p was the only concurrent miRNA in two softwares (Fig. 3a). The binding sites between circZNF83 and miR-324-5p sequences were presented in Figure 3b. The expression of miR-324-5p was upregulated by sevenfold changes after the transfection of miR-324-5p mimic contrasted to miR-NC transfection (Fig. 3c). By performing the dual-luciferase reporter assay, we found that the relative luciferase activity of circZNF83 WT group was suppressed by miR-324-5p overexpression but that of circZNF83 MUT group was unchanged (Fig. 3d,e). Also, RIP assay suggested that circZNF83 and miR-324-5p were abundant in anti-Ago2 group by comparison with the anti-IgG group (Fig. 3f,g). The overexpression of circZNF83

decreased the level of miR-324-5p in HuH-7 and HCCLM3 cells (Fig. 3h). Additionally, miR-324-5p expression was downregulated in HCC tissues and cells by contrast to normal controls (Fig. 3i,j). The qRT-PCR also manifested that GL63 treatment upregulated the miR-324-5p level in HuH-7 and HCCLM3 cells (Fig. 3k). The aforementioned data proved that miR-324-5p was a target of circZNF83.

GL63 impeded the progression of HCC by regulating the circZNF83/miR-324-5p axis. To explore whether miR-324-5p was responsible for the effect of circZNF83 on GL63 function, GL63-treated HCC cells were transfected with circZNF83, circZNF83 + miR-324-5p, or the negative controls. The qRT-PCR displayed that miR-324-5p transfection eliminated the circZNF83-induced inhibition of miR-324-5p expression in GL63-treated HuH-7 and HCCLM3 cells (Fig. 4a). The stimulative influences of circZNF83 on cell viability (Fig. 4b), colony formation (Fig. 4c), and cell cycle progression (Fig. 4d,e) were all counteracted by miR-324-5p mimic. Meanwhile, the overexpression of miR-324-5p alleviated the circZNF83-meidated apoptosis inhibition (Fig. 4f–h) and
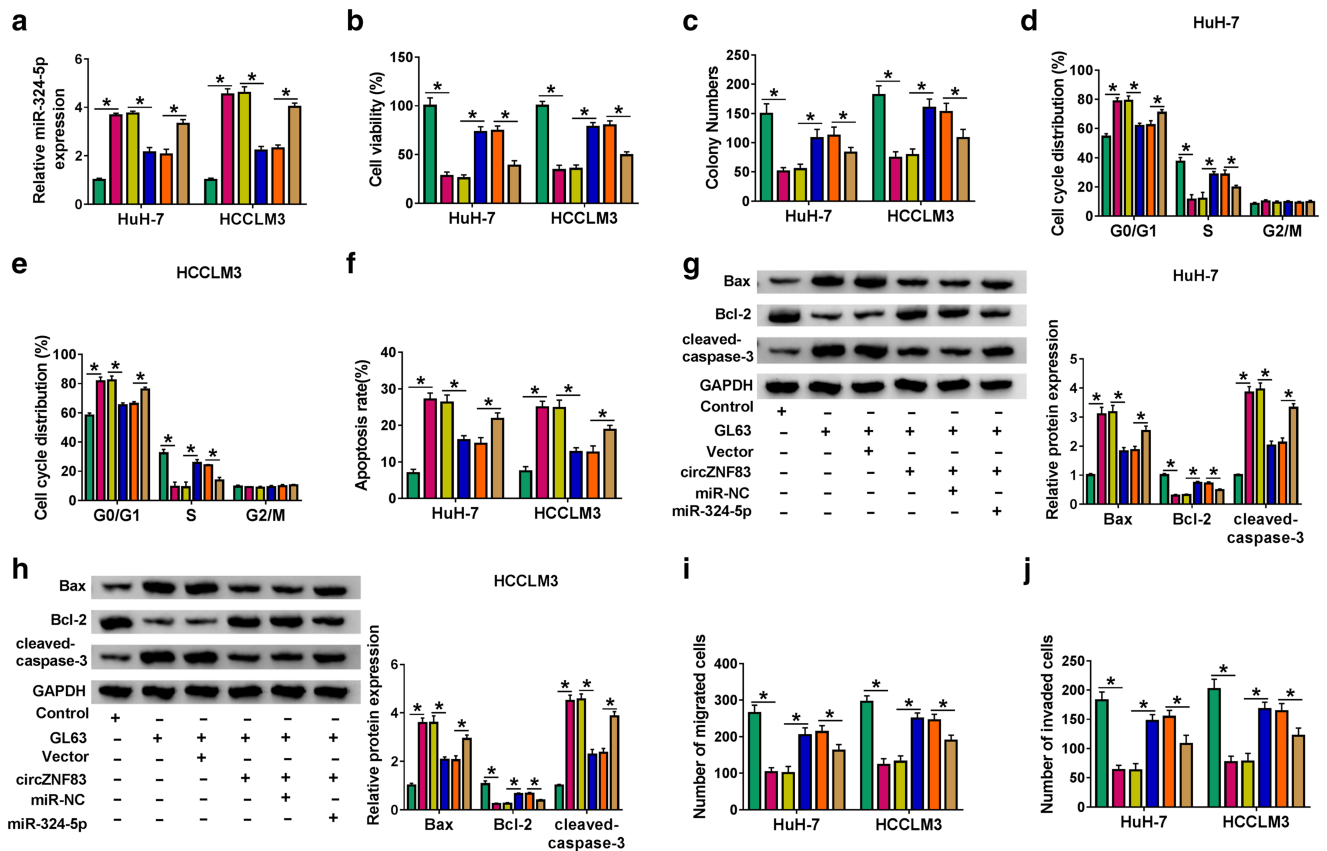

Figure 4 GL63 impeded the progression of HCC by regulating the circZNF83/miR-324-5p axis. Six groups (Control, GL63, GL63 + vector, GL63 + circZNF83, GL63 + circZNF83 + miR-NC, and GL63 + circZNF83 + miR-324-5p) were set in HuH-7 and HCCLM3 cells. (a) The level of miR-324-5p was assayed via qRT-PCR. (b) Cell viability was determined via CCK-8 assay. (c) Cell proliferation was assessed via colony formation assay. (d–f) Cell cycle (d and e) and cell apoptosis (f) were measured via flow cytometry. (g and h) The apoptosis-related proteins were detected via western blot. (i and j) Cell migration (i) and invasion (j) were examined via transwell assay. *$P < 0.05$. (a–j) ■, Control; ■, GL63; ■, GL63 + vector; ■, GL63 + circZNF83; ■, GL63 + circZNF83 + miR-NC; ■, GL63 + circZNF83 + miR-324-5p.

migration/invasion promotion (Fig. 4i,j) in GL63-induced cells. Thus, GL63 inhibited the progression of HCC by reducing circZNF83 level to upregulate miR-324-5p.

CircZNF83 affected the CDK16 expression by sponging miR-324-5p.

The starBase v2.0 predicted that the 3′UTR sequence of CDK16 contained the binding sites of miR-324-5p (Fig. 5a). The repression of luciferase activity in miR-324-5p + CDK16 3′UTR WT group (rather than miR-324-5p + CDK16 3′UTR MUT group) suggested that miR-324-5p could interact with the 3′UTR of CDK16 (Fig. 5b,c). CDK16 protein expression was reduced in miR-324-5p transfection group compared with miR-NC group (Fig. 5d), indicating the negative regulation of miR-324-5p on CDK16. The mRNA and protein levels of CDK16 were upregulated in HCC tissues (Fig. 5e,f) and cells (Fig. 5g,h) relative to the normal tissues and cells. In addition, the protein expression of CDK16 was markedly decreased after treatment of GL63 in HuH-7 and HCCLM3 cells (Fig. 5i). More interestingly, circZNF83 transfection led to a stimulative effect on the protein level of CDK16 but this regulation was mitigated by transfection of miR-324-5p (Fig. 5j,k). These results

identified that circZNF83 could sponge miR-324-5p to regulate the level of CDK16 in HCC cells.

The function of GL63 in HCC progression was partly achieved by upregulating miR-324-5p to inhibit the expression of CDK16.

GL63-induced miR-324-5p upregulation was inhibited by transfection of anti-miR-324-5p, which indicated that the inhibitory efficiency of anti-miR-324-5p was excellent (Fig. 6a). Western blot demonstrated that anti-miR-324-5p promoted the protein expression of CDK16 in GL63-treated HuH-7 and HCCLM3 cells, while the introduction of si-CDK16 signally abated this promotion (Fig. 6b). The suppressive roles of GL63 on cell viability (Fig. 6c), colony formation (Fig. 6d) and cell cycle (Fig. 6e,f) were restored by miR-324-5p inhibitor, but this restoration was subsequently repressed after the knockdown of CDK16. Through the detection of apoptotic rate (Fig. 6g) and apoptotic proteins (Fig. 6h,i), we found that si-CDK16 also ameliorated the inhibitory regulation of anti-miR-324-5p on cell apoptosis in GL63-treated cells. Transwell assay exhibited that miR-324-5p inhibitor abrogated the GL63-induced inhibition of cell migration
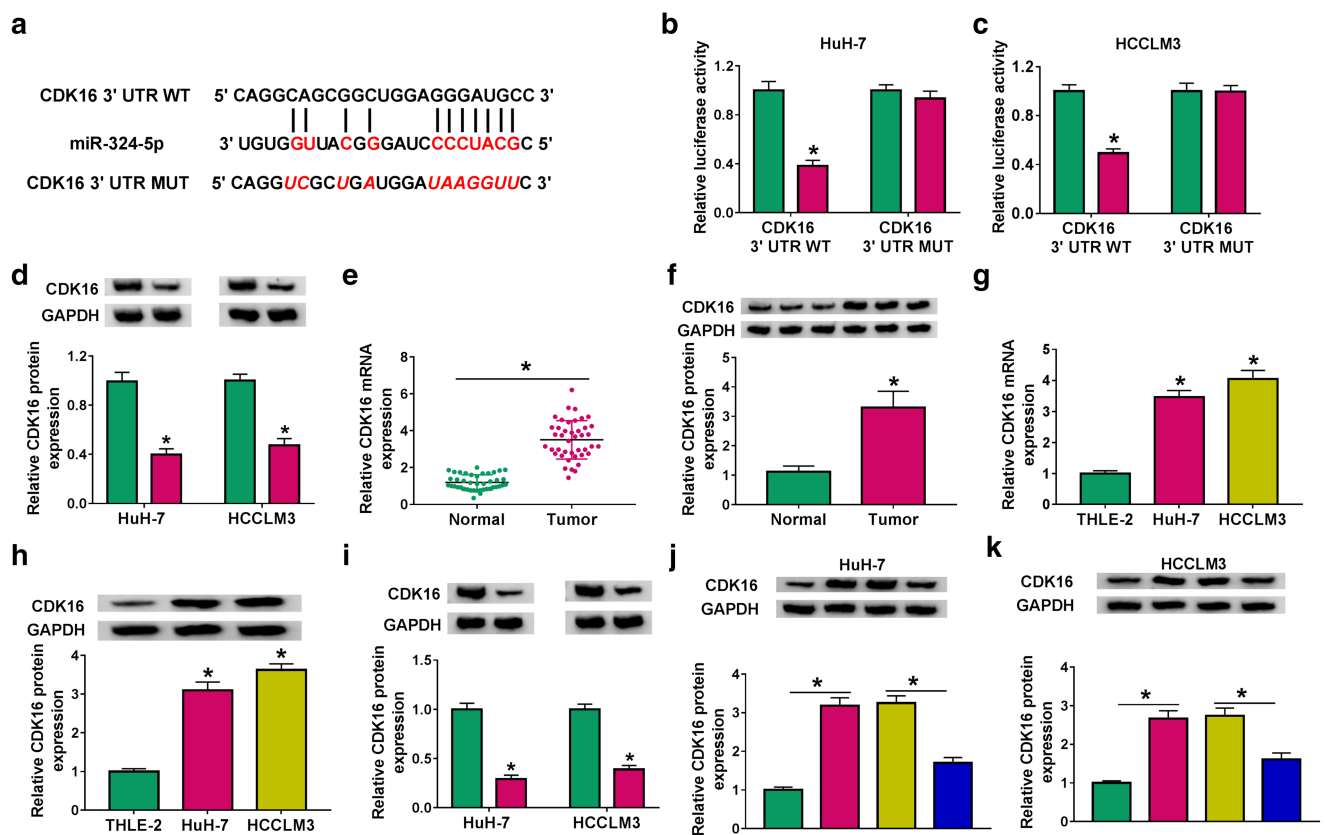

Figure 5 CircZNF83 affected the CDK16 expression by sponging miR-324-5p. (a) The binding sites between CDK16 3′UTR and miR-324-5p were predicted by starBase v2.0. (b and c) Dual-luciferase reporter assay verified that miR-324-5p interacted with the 3′UTR of CDK16. (d) CDK16 protein expression was detected by western blot after HuH-7 and HCCLM3 cells were transfected with miR-NC or miR-324-5p. (e–h) The mRNA and protein levels of CDK16 were determined by qRT-PCR and western blot in tissues (e and f) and cells (g and h). (i) Western blot was applied for protein analysis of CDK16 after treatment of GL63. (j and k) The protein level of CDK16 was assayed using western blot in vector, circZNF83, circZNF83 + miR-NC or circZNF83 + miR-324-5p group. *$P < 0.05$. (b–d) ▪, miR-NC; ▪, miR-324-5p. (i) ▪, Control; ▪, GL63. (j and k) ▪, vector; ▪, circZNF83; ▪, circZNF83 + miR-NC; ▪, circZNF83 + miR-324-5p.
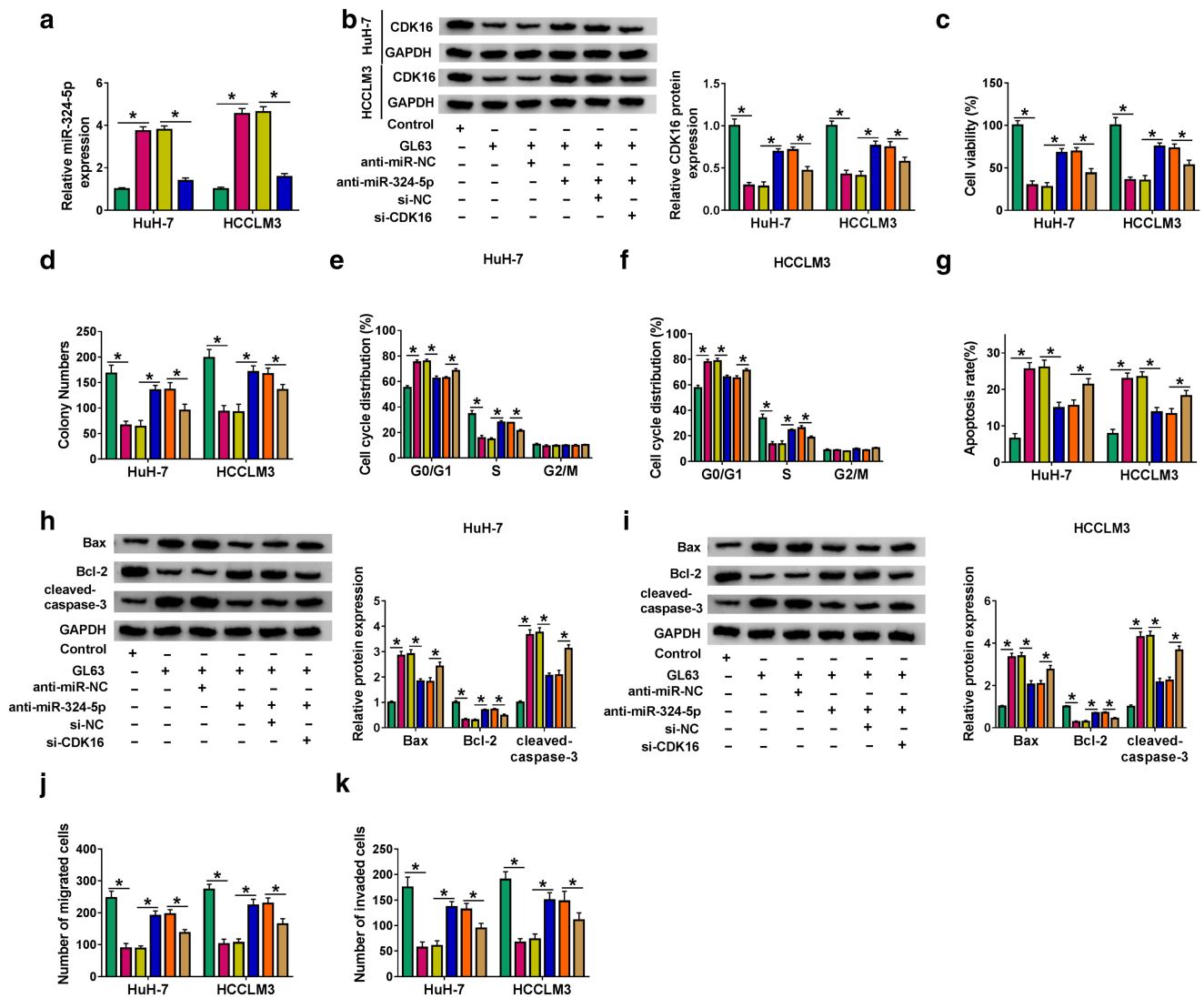
Figure 6 The function of GL63 in HCC progression was partly achieved by upregulating miR-324-5p to inhibit the expression of CDK16. (a) The qRT-PCR was performed to analyze the expression of miR-324-5p in Control, GL63, GL63 + anti-miR-NC, or GL63 + anti-miR-324-5p group. (b) Western blot was performed to assay the CDK16 protein level in HuH-7 and HCCLM3 cells transfected with anti-miR-NC, anti-miR-324-5p, anti-miR-324-5p + si-NC, or anti-miR-324-5p + si-CDK16 under the treatment of GL63. (c) CCK-8 assay was performed to detect cell viability. (d) Colony formation assay was conducted to measure the ability of cell proliferation. (e–g) Flow cytometry was conducted to evaluate cell cycle (e and f) and cell apoptosis (g). (h and i) Western blot was conducted to examine the protein levels of apoptotic markers. (j and k) Transwell assay was applied to analyze cell migration (j) and invasion (k). *$P < 0.05$. (a) ▬, Control; ▬, GL63; ▬, GL63 + anti-miR-NC; ▬, GL63 + anti-miR-324-5p. (c–k) ▬, Control; ▬, GL63; ▬, GL63 + anti-miR-NC; ▬, GL63 + anti-miR-324-5p; ▬, anti-miR-324-5p + si-NC; ▬, anti-miR-324-5p + si-CDK16.

and invasion, which was countervailed by knockdown of CDK16 (Fig. 6j,k). Taken together, miR-324-5p/CDK16 axis was also involved in the regulation of GL63 in HCC progression.

GL63 inactivated the JAK2/STAT3 signaling pathway by inhibiting the circZNF83 expression to mediate the miR-324-5p/CDK16 axis.
The previous study has stated that GL63 suppressed HCC cell proliferation by blocking the JAK2/STAT3 signaling pathway.[7] To validate the effect of GL63 on JAK2/STAT3 signaling pathway, we detected the

associated protein markers using western blot assay. As the results in Figure 7a,b, GL63 treatment downregulated the levels of p-JAK2/JAK2 and p-STAT3/STAT3 but this downregulation was counterbalanced following the overexpression of circZNF83. Therefore, GL63 inactivated the JAK2/STAT3 signaling pathway by repressing the level of circZNF83. Furthermore, the regulatory effect of circZNF83 transfection on the GL63-mediated JAK2/STAT3 signal inhibition was abrogated by miR-324-5p overexpression (Fig. S1A,B). Downregulation of miR-324-5p also mitigated the GL63-induced inhibitory influence on JAK2/STAT3 signaling pathway, whereas transfection of si-CDK16 partly

prevented the function of anti-miR-324-5p (Fig. S1C,D). All in all, GL63 blocked the JAK2/STAT3 pathway via reducing the circZNF83/miR-324-5p-mediated CDK16 expression.

GL63 reduced tumor growth by downregulating circZNF83 to block the miR-324-5p/CDK16-mediated JAK2/STAT3 signaling pathway in vivo.

The xenograft tumor model in mice revealed that tumor volume (Fig. 8a) and weight (Fig. 8b) were suppressed by GL63, while the inhibition of tumor growth was relieved by the expression upregulation of circZNF83. The excised tumor images were shown in Figure 8c. The qRT-PCR showed that circZNF83 level was higher (Fig. 8d) and miR-324-5p expression was lower (Fig. 8e) in GL63 + circZNF83 group than these in GL63 + vector group. CDK16, p-JAK2/JAK2, and p-STAT3/STAT3 protein levels were all suppressed by GL63, which was then lightened after the

overexpression of circZNF83 (Fig. 8f). All in all, GL63 inhibited tumor growth by blocking the JAK2/STAT3 signaling pathway through the circZNF83/miR-324-5p/CDK16 axis in vivo.

Discussion

GL63 exerted the tumor-suppressive effect on nasopharyngeal carcinoma to induce G2/M arrest and cell apoptosis.[21] Also, GL63 exhibits more favorable pharmacological activity than CUR to inhibit carcinogenesis in HCC.[7] Herein, we clarified that GL63 acted as an anti-tumor drug in HCC by regulating the circZNF83/miR-324-5p/CDK16 axis to block the JAK2/STAT3 signaling pathway.

Different roles of circRNAs have been revealed in diverse kinds of tumors. For example, circPLK1 contributed to cell growth and invasion in breast cancer cells by binding to miR-4500 and elevating the IGF1 expression.[22] Hsa_circ_0000658 induced the repression of proliferation and migration in osteosarcoma cells by
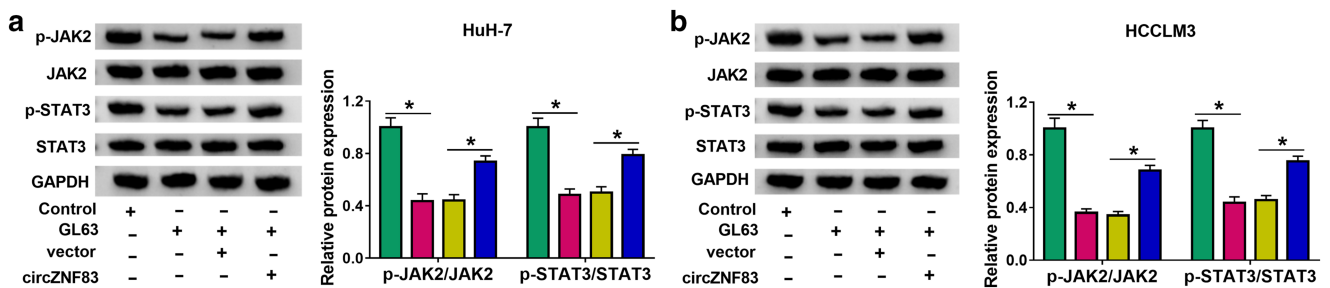

Figure 7 GL63 inactivated the JAK2/STAT3 signaling pathway by inhibiting the circZNF83 expression. (a and b) The protein levels of p-JAK2/JAK2 and p-STAT3/STAT3 were detected by western blot in Control, GL63, GL63 + vector, or GL63 + circZNF83 group. *$P < 0.05$. (a and b) ■, Control; ■, GL63; ■, GL63 + vector; ■, GL63 + circZNF83.
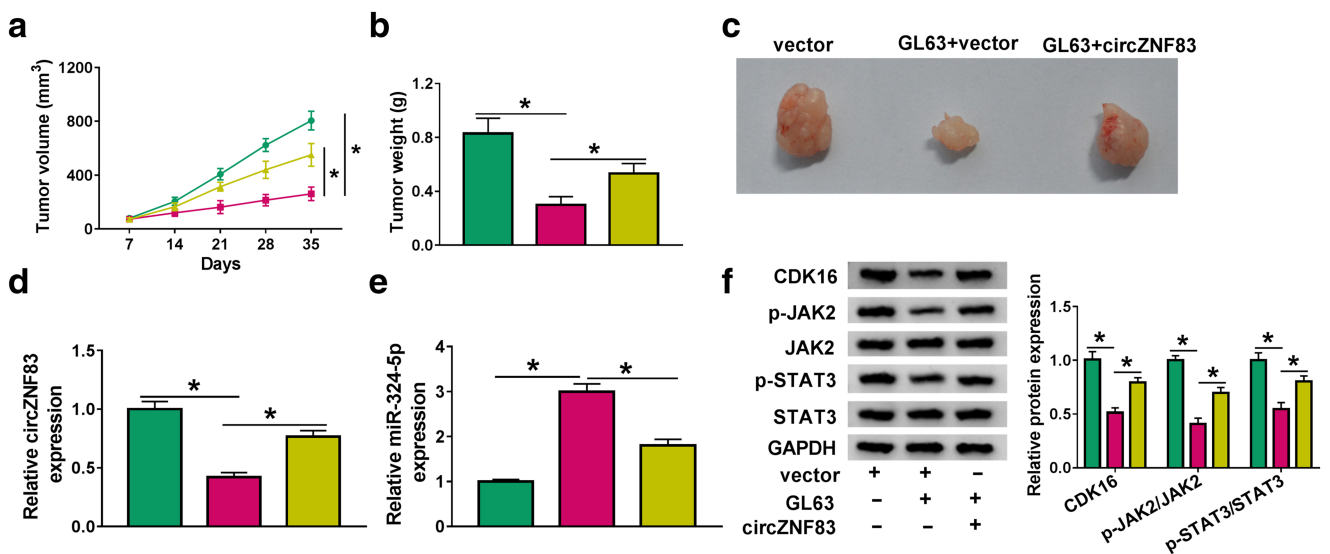

Figure 8 GL63 reduced tumor growth by downregulating circZNF83 to block the miR-324-5p/CDK16-mediated JAK2/STAT3 signaling pathway in vivo. (a and b) Tumor volume (a) and weight (b) were measured in each group. (c) Tumor pictures were photographed. (d and e) The levels of circZNF83 (d) and miR-324-5p (e) in tumor tissues were examined using qRT-PCR. (f) The protein levels of CDK16, p-JAK2/JAK2, and p-STAT3/STAT3 in tumor tissues were assayed using western blot. *$P < 0.05$. (a) ●, vector; ■, GL63 + vector; ▲, GL63 + circZNF83. (b, d–f) ■, vector; ■, GL63 + vector; ■, GL63 + circZNF83.
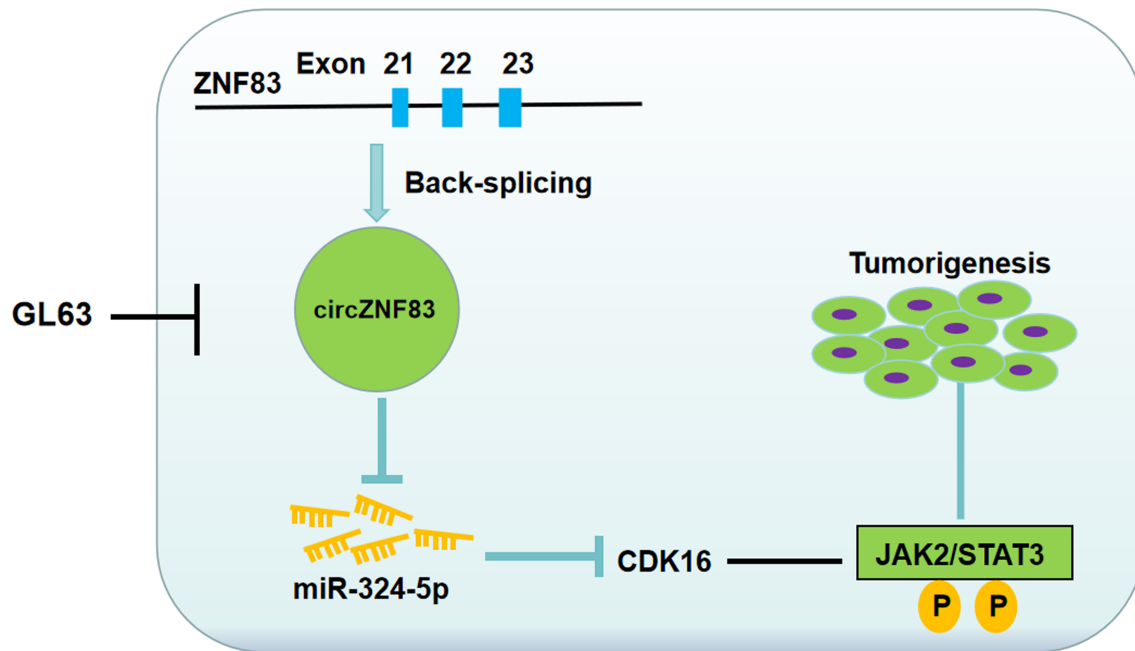
Figure 9 The figures of mechanism model in this study.

targeting the miR-1227/IRF2 axis.[23] In addition, circTMEM45A served as a miR-665 sponge to promote tumorigenesis and cell mobility in HCC by upregulating the IGF2 level.[24] Our expression analysis indicated that circZNF83 expression was downregulated in GL63-treated HCC cells relative to normal HCC cells. Further cellular experiments indicated that the upregulation of circZNF83 mitigated the GL63-mediated cell growth reduction, cell cycle arrest, cell apoptosis promotion, and cell migration/invasion repression. These findings suggested that circZNF83 functioned as a carcinogenic factor in HCC and the antitumor influences of GL63 were partly attributed to the downregulation of circZNF83 expression.

To further explore how circZNF83 affected the function of GL63 in HCC cells, the miRNA target for circZNF83 was searched by bioinformatics analysis. Circinteractome and circbank predicted that miR-324-5p was a probable miRNA target for circZNF83. Subsequently, we affirmed that circZNF83 could interact with miR-324-5p. The expression level of miR-324-5p was negatively modulated by circZNF83. Circ_0067835 has facilitated the progression of endometrial cancer by sponging miR-324-5p.[25] Circ_0079662 could act as a sponge of miR-324-5p to increase the drug resistance in colon cancer.[26] Our results also showed that circZNF83 was implicated in the functional regulation of GL63 through of the sponge effect on miR-324-5p.

The issued studies have indicated that miR-324-5p affected cancer progression by regulating the levels of downstream targets. Zhang *et al.* reported that cell metastatic ability of gallbladder carcinoma was repressed by miR-324-5p via decreasing the TGFB2 level.[27] Lin *et al.* stated that miR-324-5p accelerated cell apoptosis in gastric cancer by inducing the downregulation of TSPAN8.[28] This study identified that miR-324-5p targeted the CDK16 3ʹUTR sequence to repress the transcriptional and post-transcriptional

levels of CDK16. In addition, our data manifested that GL63 inhibited the malignant progression of HCC partly by mediating the miR-324-5p/CDK16 axis. Furthermore, circZNF83 could upregulate the CDK16 expression via targeting miR-324-5p.

JAK2/STAT3 pathway is a signal transducer and activator in tumorigenesis and development.[29] The anti-cancer function of GL63 in HCC was also achieved by inactivating the JAK2/STAT3 pathway.[7] However, it remains unclear about the regulatory mechanism of GL63 in the JAK2/STAT3 signaling pathway. In the present research, we discovered that GL63 blocked the JAK2/STAT3 pathway by depending on the circZNF83/miR-324-5p/CDK16 axis. In vivo assays also manifested that GL63 suppressed tumorigenesis of HCC by downregulating the circZNF83 level to affect the miR-324-5p/CDK16 axis and JAK2/STAT3 pathway.

This study still has some limitations. For example, the direct target of GL63 remains unclear although we have confirmed that GL63 could regulate the level of circZNF83 to affect the tumor progression of HCC. The further studies need to be performed in future. In addition, it is possible that circZNF83 can be involved in the GL63-induced anti-tumor function in HCC progression by targeting other miRNA/mRNA axes. More data and information will be interesting to improve the level of this study.

Conclusion

In conclusion, our results suggested that GL63 targeted the circZNF83/miR-324-5p/CDK16 axis to inactivate the JAK2/STAT3 pathway to act as a tumor inhibitor in HCC progression (Fig. 9). This research has provided the first-hand data to elucidate the molecular mechanism of GL63 in the regulation of HCC progression.

Data availability statement. The analyzed data sets generated during the present study are available from the corresponding author on reasonable request.

References

1 Abreu P, Ferreira R, Mineli V *et al*. Alternative biomarkers to predict tumor biology in hepatocellular carcinoma. *Anticancer Res.* 2020; **40**: 6573–784.

2 Kim E, Viatour P. Hepatocellular carcinoma: old friends and new tricks. *Exp. Mol. Med.* 2020.

3 Ashrafizadeh M, Zarrabi A, Hashemi F *et al*. Curcumin in cancer therapy: a novel adjunct for combination chemotherapy with paclitaxel and alleviation of its adverse effects. *Life Sci.* 2020; **256**: 117984.

4 Shao S, Duan W, Xu Q *et al*. Curcumin suppresses hepatic stellate cell-induced hepatocarcinoma angiogenesis and invasion through downregulating CTGF. *Oxid. Med. Cell. Longev.* 2019; **2019**: 8148510.

5 Chen Y, Lu Y, Lee RJ *et al*. Nano encapsulated curcumin: and its potential for biomedical applications. *Int. J. Nanomedicine* 2020; **15**: 3099–120.

6 Mishra S, Patel S, Halpani CG. Recent updates in curcumin pyrazole and isoxazole derivatives: synthesis and biological application. *Chem. Biodivers.* 2019; **16**: e1800366.

7 Zhao JA, Sang MX, Geng CZ *et al*. A novel curcumin analogue is a potent chemotherapy candidate for human hepatocellular carcinoma. *Oncol. Lett.* 2016; **12**: 4252–62.

8 Xiao J, Chu Y, Hu K *et al*. Synthesis and biological analysis of a new curcumin analogue for enhanced anti-tumor activity in HepG 2 cells. *Oncol. Rep.* 2010; **23**: 1435–41.

9 Wang M, Yu F, Chen X *et al*. The underlying mechanisms of noncoding RNAs in the chemoresistance of hepatocellular carcinoma. *Mol Ther Nucleic Acids* 2020; **21**: 13–27.

10 Kristensen LS, Andersen MS, Stagsted LVW *et al*. The biogenesis, biology and characterization of circular RNAs. *Nat. Rev. Genet.* 2019; **20**: 675–91.

11 Chen LL. The expanding regulatory mechanisms and cellular functions of circular RNAs. *Nat. Rev. Mol. Cell Biol.* 2020; **21**: 475–90.

12 Zhang HD, Jiang LH, Hou JC *et al*. Circular RNA hsa_circ_0052112 promotes cell migration and invasion by acting as sponge for miR-125a-5p in breast cancer. *Biomed. Pharmacother.* 2018; **107**: 1342–53.

13 Luo Z, Mao X, Cui W. Circular RNA expression and circPTPRM promotes proliferation and migration in hepatocellular carcinoma. *Med. Oncol.* 2019; **36**: 86.

14 Tang Q, Hann SS. Biological roles and mechanisms of circular RNA in human cancers. *Onco. Targets. Ther.* 2020; **13**: 2067–92.

15 Cao L, Xie B, Yang X *et al*. MiR-324-5p suppresses hepatocellular carcinoma cell invasion by counteracting ECM degradation through post-transcriptionally downregulating ETS1 and SP1. *PLoS ONE* 2015; **10**: e0133074.

16 Liu Q, Wang C, Jiang Z *et al*. circRNA 001306 enhances hepatocellular carcinoma growth by up-regulating CDK16 expression via sponging miR-584-5p. *J. Cell. Mol. Med.* 2020; **24**: 14306–15.

17 Zhu M, Shi X, Gong Z *et al*. Cantharidin treatment inhibits hepatocellular carcinoma development by regulating the JAK2/STAT3 and PI3K/Akt pathways in an EphB4-dependent manner. *Pharmacol. Res.* 2020; **158**: 104868.

18 Zhao Z, Song J, Tang B *et al*. CircSOD2 induced epigenetic alteration drives hepatocellular carcinoma progression through activating JAK2/STAT3 signaling pathway. *J. Exp. Clin. Cancer Res.* 2020; **39**: 259.

19 Xiao J, Tan Y, Pan Y *et al*. A new cyclooxygenase-2 inhibitor, (1E,4E)-1,5-bis(2-bromophenyl)penta-1,4-dien-3-one (GL63) suppresses cyclooxygenase-2 gene expression in human lung epithelial cancer cells: coupled mRNA stabilization and posttranscriptional inhibition. *Biol. Pharm. Bull.* 2010; **33**: 1170–5.

20 Lai J, Xin J, Fu C *et al*. CircHIPK3 promotes proliferation and metastasis and inhibits apoptosis of renal cancer cells by inhibiting MiR-485-3p. *Cancer Cell Int.* 2020; **20**: 248.

21 Pan Y, Xiao J, Liang G *et al*. A new curcumin analogue exhibits enhanced antitumor activity in nasopharyngeal carcinoma. *Oncol. Rep.* 2013; **30**: 239–45.

22 Lin G, Wang S, Zhang X *et al*. Circular RNA circPLK1 promotes breast cancer cell proliferation, migration and invasion by regulating miR-4500/IGF1 axis. *Cancer Cell Int.* 2020; **20**: 593.

23 Jiang X, Chen D. Circular RNA hsa_circ_0000658 inhibits osteosarcoma cell proliferation and migration via the miR-1227/IRF2 axis. *J. Cell. Mol. Med.* 2020.

24 Zhang T, Jing B, Bai Y *et al*. Circular RNA circTMEM45A acts as the sponge of microRNA-665 to promote hepatocellular carcinoma progression. *Mol Ther Nucleic Acids* 2020; **22**: 285–97.

25 Liu Y, Chang Y, Cai Y. Circ_0067835 sponges miR-324-5p to induce HMGA1 expression in endometrial carcinoma cells. *J. Cell. Mol. Med.* 2020.

26 Lai M, Liu G, Li R *et al*. Hsa_circ_0079662 induces the resistance mechanism of the chemotherapy drug oxaliplatin through the TNF-α pathway in human colon cancer. *J. Cell. Mol. Med.* 2020; **24**: 5021–7.

27 Zhang X, Zhang L, Chen M *et al*. miR-324-5p inhibits gallbladder carcinoma cell metastatic behaviours by downregulation of transforming growth factor beta 2 expression. *Artif. Cells Nanomed. Biotechnol.* 2020; **48**: 315–24.

28 Lin H, Zhou AJ, Zhang JY *et al*. MiR-324-5p reduces viability and induces apoptosis in gastric cancer cells through modulating TSPAN8. *J. Pharm. Pharmacol.* 2018; **70**: 1513–20.

29 Jaskiewicz A, Domoradzki T, Pajak B. Targeting the JAK2/STAT3 pathway—Can we compare it to the two faces of the God Janus? *Int. J. Mol. Sci.* 2020; **21**: 8261.

Supporting information

Additional supporting information may be found online in the Supporting Information section at the end of the article.

Fig. S1. GL63 inactivated the JAK2/STAT3 signaling pathway by regulating the circZNF83/miR-324-5p/CDK16 axis. (A-D) The p-JAK2/JAK2 and p-STAT3/STAT3 levels were examined by western blot in Control, GL63, GL63 + vector, GL63 + circZNF83, GL63 + circZNF83 + miR-NC or GL63 + circZNF83 + miR-324-5p group (A-B) and Control, GL63, GL63 + anti-miR-NC, GL63 + anti-miR-324-5p, GL63 + anti-miR-324-5p + si-NC or GL63 + anti-miR-324-5p + si-CDK16 group (C-D) in HuH-7 and HCCLM3 cells. $*P < 0.05$.